

Improving the Classical Geophone Sensor Element by Digital Correction

Rune Brincker
Aalborg University, Denmark, rb@svibs.com

Thomas L. Lagö
Pinocchio Data Systems, Denmark, tl@pidats.com

Palle Andersen
Structural Vibration Solutions, Denmark, pa@svibs.com

Carlos Ventura
University of British Columbia, Canada, ventura@civil.ubc.ca

ABSTRACT

Geophones are highly sensitive motion transducers that have been used by seismologists and geophysicists for decades. The conventional geophone's ratio of cost to performance, including noise, linearity and dynamic range is unmatched by advanced modern accelerometers. However, the problem of this sensor is that it measures velocity, and that the linear frequency range is limited to frequencies above the natural frequency, typically at 4-12 Hz. It is shown in this paper how the sensor signal can be digitally linearized 2 decades below the natural frequency obtaining a sensor that allows the user to measure displacement, velocity or acceleration with high sensitivity and large dynamic range.

NOMENCLATURE

$x(t)$	base displacement
$y(t)$	coil displacement
M	moving mass
k	suspension stiffness
c	suspension damping ratio
f	frequency
ω	cyclic frequency
ζ	damping ratio
H	transfer function
V	voltage
G	transduction constant

INTRODUCTION

The geophone sensor is in principle a very simple sensor. In its simplest form, it is just a coil suspended around a permanent magnet - just like a loud speaker coil/magnet system. When the coil moves relative to the magnet, a voltage is induced in the coil according to the Faraday law that we all have investigated during our high school days: think back to when you were sitting with a permanent magnet moving it inside a coil and looking at the dial gage moving. The induced voltage is proportional to the relative speed, thus the geophone sensor element is measuring velocity.

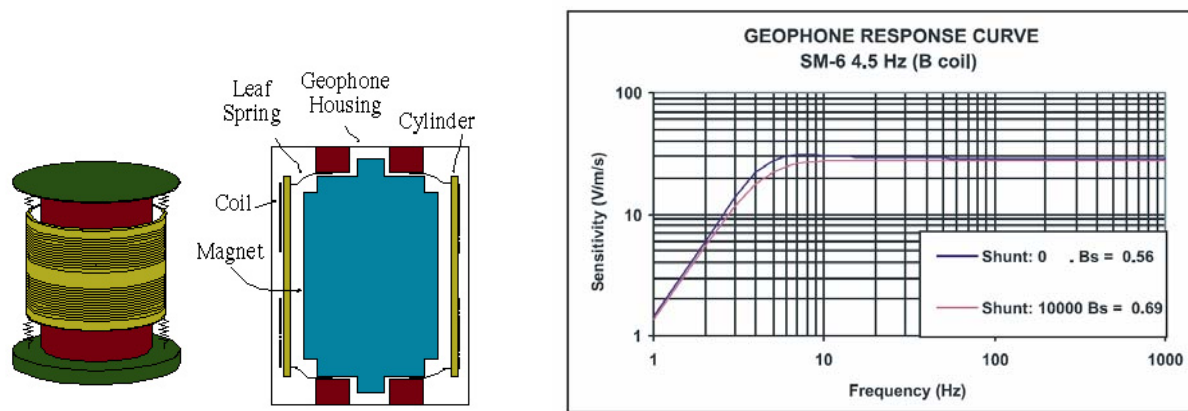


Figure 1. Left: An isometric and cross-sectional view of a typical geophone, after Aaron Barzilai [1], Right: Frequency response of the SM-6 geophone sensor element from I-O, see [4] used in the Pinocchio A 150 Vibraphone

This sensor type has several advantages. Because of the simple construction, the sensor element is robust and cheap. The sensor is simple to use because it is a passive sensor element that does not require any kind of power supply. Further, if the sensor is well engineered, it has an excellent linearity and a large frequency range. Since normally not only a single coil is used, but two coils in differential coupling, and since the sensor does not include any active elements to introduce potential additional noise, the sensor has an extremely low noise floor.

However, there are some drawbacks with this type of sensor design. The sensor has two main weak points: a) limited excursion, b) limited frequency response. The limited excursion is due to the fact that the coil can only move a certain amount relatively to the permanent magnet; this normally restricts the relative coil movement to a few mm. The limited frequency response is due to the fact that since the coil is suspended by a spring system, the system properties change around the natural frequency of the suspension system. The natural frequency of a typical geophone sensor element is around 4-14 Hz. Above the natural frequency the sensor element has its nice properties giving a signal according to the specifications provided by the vendor. However, below the natural frequency the response is rolling off. An overview of the sensor element design and a typical transfer function is given in Figure 1.

Recently a successful attempt has been made to improve the geophone sensor element, Barzilai [1]. The main idea relative to Barzilai's work is to improve the response of the sensor by adding a separate displacement measurement to improve the response in the low frequency region, Barzilai et al, [2].

The idea of the work presented herein, is based on the idea of using the geophone sensor element as it is. The idea is, that since the noise properties of the sensor element is so fine, all the needed information is already available, and thus, no additional information has to be added. However, since the information in the low frequency region is distorted by the limited response of the geophone, the signal in the low frequency region is recovered by basically inverting the frequency response of the geophone element, often referred to as inverse filtering. This can be done by using a frequency response function common for all sensor elements of a given type, or better; to use a frequency response function individually calibrated for each sensor element.

The investigations in this paper is performed on the Pinocchio A 150 sensor, see Figure 2 and Ref. [3]. The Pinocchio sensor is based SM-6 geophone sensor element from I-O, inc, Ref. [4]. The Pinocchio sensor is delivered with a software routine performing the described corrections and integrations/differentiations. Thus the more general application of the sensor to obtain either displacement, velocity and acceleration in a broader frequency range justifies the name "Vibraphone" – the Pinocchio A 150 Vibraphone. The key concepts of the Pinocchio A 150 presented in this paper is protected by pending patents.

This paper will present how an effective and accurate correction algorithm can be implemented using the Discrete Fourier Transform (DFT), Brigham [3]. The reason for using the DFT is that in the frequency domain it is easier to

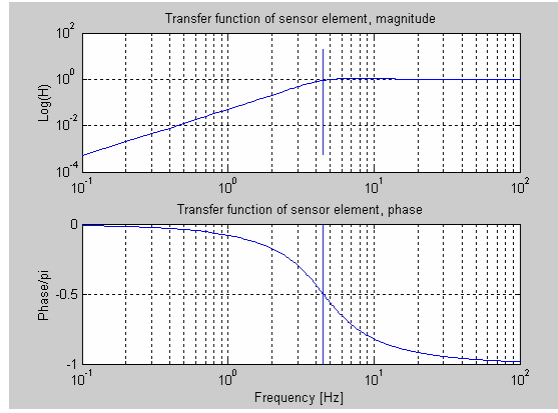
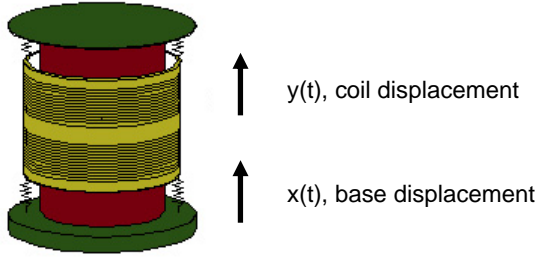


Figure 2. Left: Definition of base and coil displacements, Right: Theoretical transfer function for the Pinocchio A 150Vibraphone sensor as estimated by Eq. (5).

implement general frequency response recovery as well as integration/differentiation and general filtering, as compared to the time domain that involves convolution.

Finally, in this paper it is shown how the low frequency response of the sensor element can be accurately obtained using a laser, since the laser has a simple frequency characteristic that can be accurately accounted for.

SENSOR ELEMENT RESPONSE

It is known that the geophone sensor element is well modeled by a single degree of freedom system (1DOF), Barzilai [1], [2]. The response of the system is given by the common solutions to the “foundation displacement input and displacement output” as given for instance by Bendat and Piersol [4]. If the base and coil displacements are defined as shown in Figure 2, then the total force on the moving coil is given by

$$(1) \quad F = (x - y)k + (\dot{x} - \dot{y})c$$

Where k and c is the stiffness and damping of the suspension system. Thus the equation of motion is given by

$$(2) \quad \begin{aligned} M\ddot{y} &= (x - y)k + (\dot{x} - \dot{y})c \\ M\ddot{y} + c\dot{y} + ky &= c\dot{x} + kx \end{aligned}$$

Taking the Fourier Transform and introducing the natural frequency and the damping ratio

$$(3) \quad \begin{aligned} \omega_0 &= \sqrt{\frac{k}{M}} \\ \zeta &= \frac{c}{2\sqrt{kM}} \end{aligned}$$

we obtain the Fourier transforms X, Y of the base and coil response. According to the Faraday law, the introduced voltage is proportional to the relative speed between the coil and the magnet

$$(4) \quad V = G(\dot{y} - \dot{x})$$

where G is the transduction constant. Thus, the transfer function between the velocity of the base and the output signal of the sensor element is

$$\begin{aligned}
(5) \quad H &= \frac{Y - X}{X} = \frac{Y}{X} - 1 \\
&= \frac{\omega_0^2 + 2j\omega_0\omega\zeta}{\omega_0^2 + 2j\omega_0\omega\zeta - \omega^2} - 1 \\
&= \frac{\omega^2}{\omega_0^2 + 2j\omega_0\omega\zeta - \omega^2} = H_0
\end{aligned}$$

Surprisingly enough this transfer function is the same as the transfer function between force and displacement of the simple 1DOF system with the modification given by the factor ω^2 instead of the normal factor $1/k$, Bendat & Piersol [4]. However, because of the factor ω^2 , instead of defining a low pass filter as the traditional 1DOF system, in this case the system defines a high pass filter. The transfer function for typical values of the natural frequency and the damping ratio is shown in Figure 2. Please note that even though amplitude errors are small, as soon as the input frequency is higher than the natural frequency of the sensor element, this is not the case for the phase errors. As it appears from Figure 2, significant phase errors are present even at 20-30 Hz. This illustrates the need of correcting the sensor for amplitude and phase errors. Please also note that from Eq. (5) the following results for the phase φ can be obtained at the natural frequency $\omega_0 = 2\pi f_0$

$$\begin{aligned}
(6) \quad \varphi &= \pi/2 \\
\frac{d\varphi}{df} &= \frac{1}{f_0}
\end{aligned}$$

These relations will be used later for identification of natural frequency and damping of the sensor element. The SM-6 sensor element from I-O has the following mean properties, $G = 28.8 \text{ Vs/m}$, $f_0 = 4.5 \text{ Hz}$, $\zeta = 0.56$

DIGITAL RESPONSE IMPROVEMENT

The measured data $\dot{u} = \dot{y} - \dot{x}$ are taken from the discrete time domain to the discrete frequency domain by the Fast Fourier Transform (FTT), Brigham [3]. In the frequency domain the measured signals are easily corrected using the inverse transfer function given by Eq. (5)

$$(7) \quad \dot{X} = \dot{U} / H_0$$

and the corresponding time signals are then obtained by an inverse FFT transform. However, since the FFT is assuming periodic signals, leakage errors are introduced in this calculation procedure. Leakage is minimized by increasing the size of each data segment that originally includes N points to include βN points. The so defined segment of data is at the ends of each calculation segment appended with $\beta N / 2$ points over which a window is also applied to minimized leakage errors. Thus leakage is minimized both by increasing the effective length of the data segment and by applying an appropriate window.

If Δf is the smallest frequency needed to include in the correction procedure, and if ΔT is the sampling interval, then the minimum number of points in the data segments is given by

$$(8) \quad N = \frac{1}{\Delta f \Delta T}$$

and thus, the minimum time delay T_d between the uncorrected and the corrected signal is given by

$$(9) \quad T_d = N(1 + \beta/2)\Delta T = \frac{1 + \beta/2}{\Delta f}$$

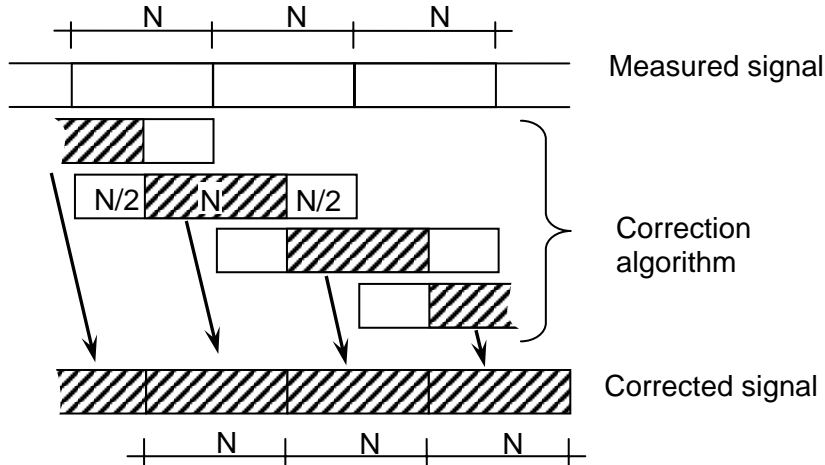


Figure 3. FFT algorithm for real time calculation of the corrected signals for $\beta = 2$.

In the same calculation procedure a general filter is easily implemented with the transfer function H_f by using the alternative formula

$$(10) \quad \dot{X} = \dot{U}H_f / H_0$$

or integration and differentiation can be implemented to obtain displacement and acceleration using the following expressions

$$(11) \quad X = \dot{X} / (j\omega)$$

$$\ddot{X} = j\omega\dot{X}$$

NOISE PROPERTIES

I-O Inc. is specifying the noise floor in the frequency domain to $\dot{U}_{noise} = 0.1 \text{ nm} / \text{s}\sqrt{\text{Hz}}$ corresponding to an electrical signal of $V_{noise} = 3 \text{ nV} / \sqrt{\text{Hz}}$. However, noise might be introduced by external sources such as electromagnetic radiation and/or air pressure fluctuations. Both sources can significantly increase the noise floor. For instance in Streickeisen et al [5] it is stated, that if the active mass is not protected against air pressure fluctuations, buoyant forces from air pressure fluctuations will at least be three orders of magnitude larger than seismic background noise.

However, since the Pinocchio sensor is protected from external electromagnetic radiation, since there are no electrical components present inside the sensor casing to produce noise, and finally since the sensor element is completely protected against air pressure fluctuations by a specially designed air tight (and water tight) casing, thus minimizing any additional noise exposure. Also, the Pinocchio sensor casing consist of an aluminum casing filled with a special epoxy compound with improved electrical conductivity. The epoxy compound is improving the protection against both air pressure fluctuations and external electromagnetic radiation. The noise floor given by I-O is assumed to be constant for all frequencies. Thus, the velocity resolution of the corrected sensor is given by

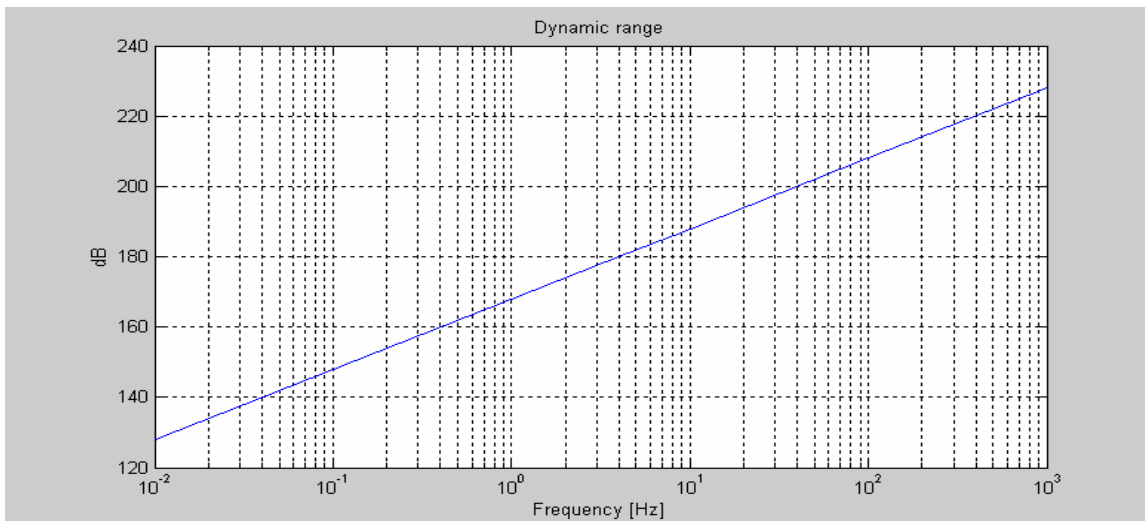


Figure 4. Dynamic range estimated for the Pinocchio A 150 sensor with digital correction.

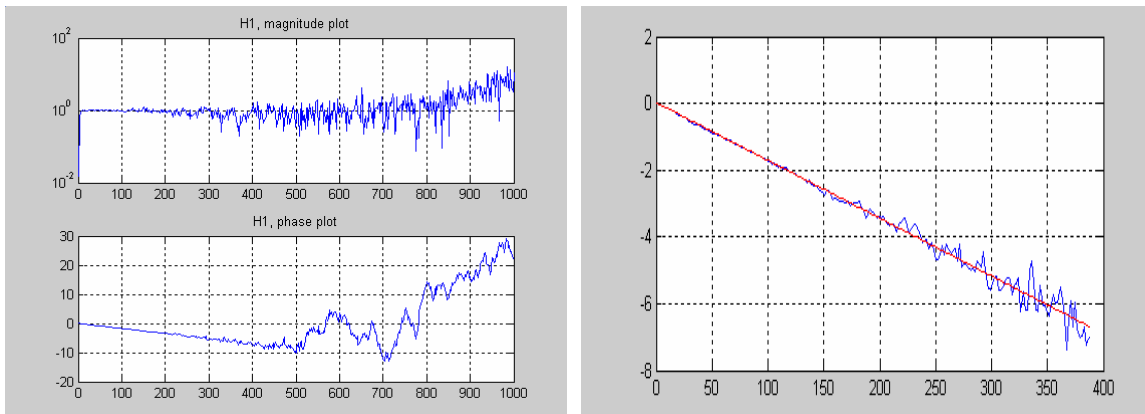


Figure 5. Left: laser calibrated versus the accelerometer, note the linear trend of laser phase error up to about 400 Hz. Right: fitting of linear trend to obtain laser delay. Phase errors in degrees.

Table 1. Maximum values and noise floor values for displacement, velocity and acceleration measurements

Quantity		Frequency [Hz]						
		0.01	0.1	1	4.5	10	100	1000
X_{\max}	$[m / \sqrt{Hz}]$	810	8.1	8.0e-2	4.5e-3	3.8e-3	4e-3	4e-3
X_{noise}	$[nm / \sqrt{Hz}]$	3.2e5	3.2e2	3.2e-1	4.0e-3	1.5e-3	1.6e-4	1.6e-5
\dot{X}_{\max}	$[m / (s\sqrt{Hz})]$	51	5.1	0.50	0.13	0.24	2.5	25
\dot{X}_{noise}	$[nm / (s\sqrt{Hz})]$	2.0e4	200	2.0	0.11	0.09	0.10	0.10
\ddot{X}_{\max}	$[m / (s^2\sqrt{Hz})]$	3.2	3.2	3.1	3.6	15	1.6e3	1.6e5
\ddot{X}_{noise}	$[nm / (s^2\sqrt{Hz})]$	1300	130	13	3.2	5.9	63	630
Dynamic range D [dB]		128	148	168	181	188	208	228

Table 2. Estimated values for natural frequency and Damping ratio

	Natural Frequency [Hz]	Damping ratio [%]
Vendor values	4.5	56
Vibraphone 1	4.62	55.1
Vibraphone 2	4.80	51.1

$$(12) \quad \dot{X}_{noise} = \dot{U}_{noise} / H_0$$

resulting in

$$(13) \quad X_{noise} = \dot{U}_{noise} / (H_0 j\omega)$$

$$\ddot{X}_{noise} = j\omega \dot{U}_{noise} / H_0$$

The maximum input signal is determined by the limited excursion of the suspended coil. For the considered sensor element, the value of the maximum excursion is $e_{max} = 4mm$. The maximum input is then found from

$$(14) \quad X_{max} H_0 = e_{max}$$

and the maximum signal-to-noise ratio R can be obtained together with the dynamic range D to

$$(15) \quad R = \frac{|X_{max}|}{|X_{noise}|} = \frac{\omega e_{max}}{\dot{U}_{noise}}$$

$$D = -20 \log(R)$$

Thus, since both the maximum input and the noise floor is similarly affected by the transfer function, the signal-to-noise ratio becomes independent of the transfer function. Further, since the noise floor is assumed constant in the frequency domain for the velocity measurement, and since the maximum value is defined as a displacement, the signal-to-noise ratio becomes proportional to frequency. This means the higher the frequency, the higher the signal-to-noise ratio. On the other hand, the signal-to-noise ratio vanishes at DC. This result – that is general and independent of what kind of signal being measured, being its displacement, velocity or acceleration - is illustrated in Figure 4. Some main results for noise floor and maximum input values are given in Table 1.

As demonstrated, this newly developed sensor has extraordinary high dynamic range. Its resolution for acceleration in the range $[1:10]Hz$ is better than $1ng/\sqrt{Hz}$, and its best resolution for velocity is

$0.1nm/(s\sqrt{Hz})$ for frequencies higher than the natural frequency, and finally its best resolution for displacement is much better than nm/\sqrt{Hz} in the high frequency band. However, these features can only be realized to the extend where the applied measurement unit can match the sensor noise properties, i.e. the noise in the measurement system must be smaller than the noise from the sensor. Thus, using measurement systems with higher noise floors will decrease the observed resolution of the sensor accordingly. For instance, if a velocity is measured with a measurement unit with an input noise floor of $100nV/\sqrt{Hz}$, then the noise floor is increased by a factor 33, and thus, the effective dynamic range is decreased by about 30 dB.

As it appears, the velocity resolution at $0.01Hz$ is $20\mu m/(s\sqrt{Hz})$, which is comparable to background seismic noise. Since soft soil sites and structures placed on the soil will amplify the vibrations around the natural frequency of the site or structure, and thus cause a significantly higher vibration level, the A 150 Vibraphone can be used for measuring ambient vibrations in soils and structures down to about $0.01Hz$.

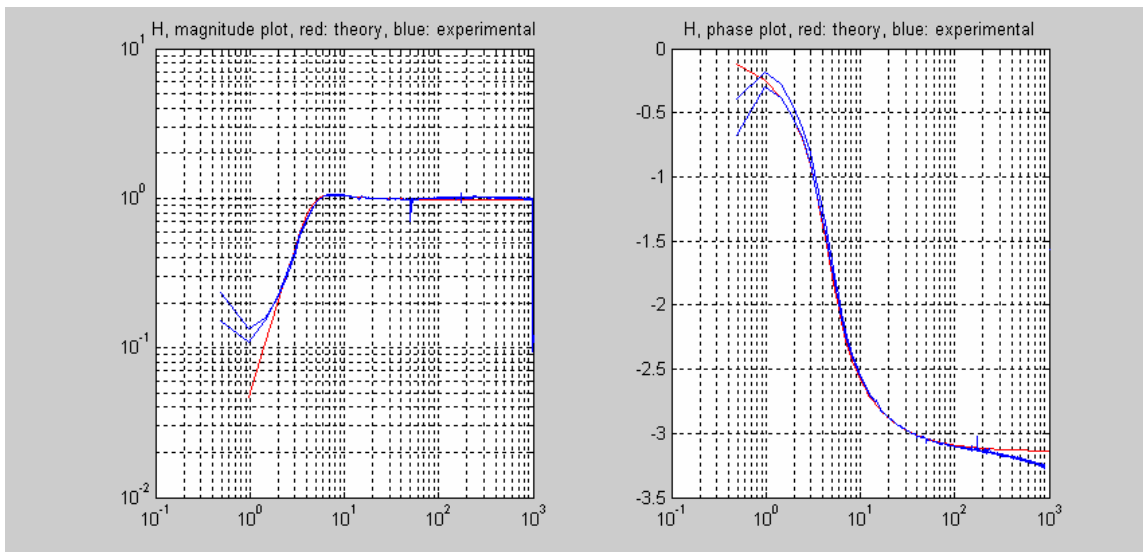


Figure 6. Empirical transfer functions for the two Pinocchio A 150 Vibraphones compared with the theoretical transfer function.

CALIBRATION

The Pinocchio A 150 sensor is calibrated in a Brüel & Kjær shaking table (BK 4802 exciter body with BK 4818 table head driven by power amplifier BK 2708) using pink noise input from a Brüel & Kjær BK 1405 noise generator. The response of the sensor is measured using a Teac, LX 10 recorder. The movement of the shaker head is measured in the high frequency range using a Brüel & Kjær 4508 B accelerometer, and in the low frequency range using an optical displacement sensor based on a laser principle.

The accelerometer response is nearly distortion free in the frequency interval from 10 to 1000 Hz, thus the distortion in this region due to accelerometer phase and amplitude errors is ignored. The laser, however, has a constant time delay between input (head displacement) and output. Calibrating the laser against the accelerometer to estimate the phase error, it is clearly seen as a linearly increasing phase error as shown in Figure 5. The linear phase error is seen to be present up to about 400 Hz. For higher frequencies the laser signal becomes buried in noise and thus, the phase error start showing random fluctuations. However, fitting the linear part of the phase error estimates a time delay in the laser of $\Delta t = 2.75 \text{ ms}$, see Figure 5, right.

After correcting the laser signal for phase errors dividing with the laser transfer function

$$(16) \quad H_{la}(f) = \exp(-i2\pi\Delta t f)$$

the empirical transfer function of the sensor can be estimated. In this case two vibraphones were investigated, Vibraphone1 and Vibraphone 2, see the estimated transfer functions compared with the theoretical transfer function in Figure 6. As it appears the response is nice and flat from the natural frequency up to the 1 kHz. Around the natural frequency, large phase errors are present, and the amplitude start rolling off. However, in accordance with a wish to limit the movements of the head of the shaking table, the input is limited to frequencies above 1 Hz. Thus, below about 1 Hz the estimated transfer function gets indeterminate due to noise. However, as it appear from Figure 6, the phase of the transfer function is well defined around the natural frequency of the sensor, and thus, a sound basis for estimating the natural frequency and the damping ratio of the sensor element based on the relations given by Eq. (6) has been established.

Fitting a straight line to the estimated phase relation in the vicinity of $\varphi = -\pi/2$ then allows the estimation of both natural frequency and damping as indicated by Eq. (6). The results for the two investigated sensors are shown in Table 2.

ACKNOWLEDGEMENTS

The authors gratefully acknowledge important advice and inspiration from Professor J.H. Thomas Schmidt, Hochschule Magdeburg Stendal, Germany and Dr. Dieter Heiland, Ingenieurbuero Dr. Heiland, Bochum, Germany.

REFERENCES

- [1] Aaron Barzilay: Improving a Geophone to Produce an Affordable broadband Seismometer. Ph.D. Thesis, Mechanical engineering, Stanford University, January 2000.
- [2] Aaron Barzilay, Tom VanZandt and Tom Kenny: Improving the Performance of a Geophone Through Capacitive Positioning Sensing and Feedback, In Proc. Of the ASME International Congress, winter, 1998.
- [3] Data sheet from Pinocchio Data Systems on the A 150 Vibraphone, on web site www.pidats.dk.
- [4] Data sheet from I-O Inc. on the SM-6 geophone sensor element, on web site www.i-o.com.
- [5] Oran Brigham: the Fast Fourier Transform, Prentice_Hall, Inc. Englewood Cliffs, N.J. 1974.
- [6] Streickeisen et al: The Leaf-Spring Seismometer: Design and Performance, Bull. Seismo. Soc. Of America, Vol. 72, No. 6, pp. 2352, December 1982
- [7] Julius Bendat and Allan Piersol: Random Data, Analysis and measurement procedures, John Wiley & Sons, Inc, 2nd edition, 1986.